A Study of LED Nonlinearity Effects on Optical Wireless Transmission using OFDM

Citation for published version:
Elgala, H, Mesleh, R & Haas, H 2009, A Study of LED Nonlinearity Effects on Optical Wireless Transmission using OFDM. in Proceedings of IEEE Conference on Wireless and Optical Communications Networks (WOCN2009).

Document Version:
Peer reviewed version

Published In:
Proceedings of IEEE Conference on Wireless and Optical Communications Networks (WOCN2009)

A Study of LED Nonlinearity Effects on Optical Wireless Transmission using OFDM

Hany Elgala†, Raed Mesleh† and Harald Haas†*

†Jacobs University Bremen, Campus Ring 1, 28759 Bremen, Germany, Email: h.elgala & r.mesleh@jacobs-university.de

*Institute for Digital Communications, The University of Edinburgh, Edinburgh EH9 3JL, UK, Email: h.haas@ed.ac.uk

***Abstract*—Orthogonal frequency division multiplexing (OFDM) is a promising technique to realize high-speed indoor optical wireless (OW) links through the exploitation of the high peak-to-average power ratio (PAPR) for intensity modulation (IM). However, non-linear distortions in the transmission chain can significantly compromise the performance of OFDM as they incur inter-channel interference. The light emitting diode (LED) is the main source for such distortions due to its nonlinear behavior. Distortion levels can be controlled when the LED operates in a quasi-linear segment of its characteristic around a bias point. The severity of non-linear distortions and the dependence of the bias point on the chosen digital modulation scheme are analyzed in this paper. In this context, the bit-error performance is determined as a function of the bias point and the applied power back-offs.**

***Index Terms*—OFDM, LED, optical wireless communication, nonlinearity distortion, PAPR.**

I. Introduction

OFDM is used in several applications such as the wireless local area network (WLAN) radio interfaces IEEE 802.11a/g/b/n due to its high spectrum efficiency and robustness against multipath effects [1]. However, the OFDM signal envelope with its high PAPR is still a design challenge. High peak signal values in OFDM stem from the superposition of a large number of usually statistically independent sub-channels that can constructively sum up to high signal peaks in the time domain. Therefore, the OFDM signal suffers from significant in-band and out-of-band distortions due to nonlinearities introduced at the transmitter. The in-band component determines the system bit-error ratio (BER) degradation [2], whereas the out-of-band component affects adjacent frequency bands [3].

In radio frequency (RF) communication, the main component that causes 'nonlinear' distortions is the transmit power amplifier (PA) (depicted in Fig. 1(a)) which is linear only over a small range of input amplitudes. In addition, signal clipping at the PA saturation level is a critical source of distortion, specially for OFDM with its high PAPR [4]. Backing-off the average power of the input signal ensures that the PA operates in its linear region and avoids saturation. Alternatively, the reduction of the PAPR through methods such as clipping and filtering, constrained coding, and selective mapping are considered [5]. However, neither power back-off nor PAPR reduction techniques necessarily mean an improvement in system performance and trade-offs must be considered. Amplifier power back-off might result in a significant power efficiency penalty and can significantly compromise signal coverage [6].

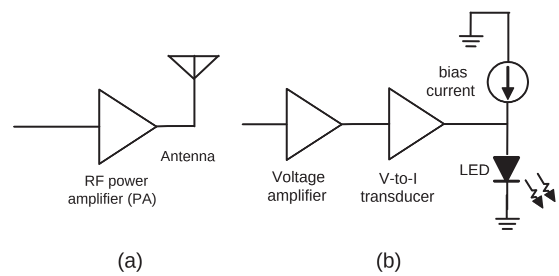

Fig. 1. The PA is the last stage driving the antenna. The LED is biased before applying the OFDM signal for intensity modulation.

PAPR reduction techniques increase the system complexity and/or sacrifice bandwidth efficiency [7, 8].

OW communication is an attractive approach to complement RF based systems for the realization of broadband access. It has many advantages such as, almost unlimited bandwidth, license-free operation, avoidance of electrosmog, and low-cost front ends and expected high data rates [9, 10]. In different studies, it is shown that OFDM can unfold it advantages also for the use in OW transmission systems [11–14]. Most importantly, it effectively combats multipath fading, and, thus, avoids inter-symbol-interference (ISI). In optical systems, the real value baseband OFDM signal is modulated onto the instantaneous power of the optical carrier resulting in IM. Since, however, optical intensity cannot be negative, the LED has to be biased (see Fig. 1(b)). The biasing point should be carefully selected to consider the maximum allowable forward current and minimize signal clipping and magnitude distortion. In addition, signal power back-offs can be used to minimize distortion levels by operating the LED in a quasi-linear segment of its characteristic around the chosen bias point as shown in Fig. 2.

The error vector magnitude (EVM) and the BER are used to measure the effect of the non-linear distortions. The effect of the bias point and the applied power back-off on the bit-error performance for several modulation orders is investigated. The rest of the paper is organized as follows. In Section II, the OFDM system model is introduced and the integration of the LED characteristics into the simulation model is explained. Simulation results are presented and discussed in Section III. Finally, Section IV concludes the paper.

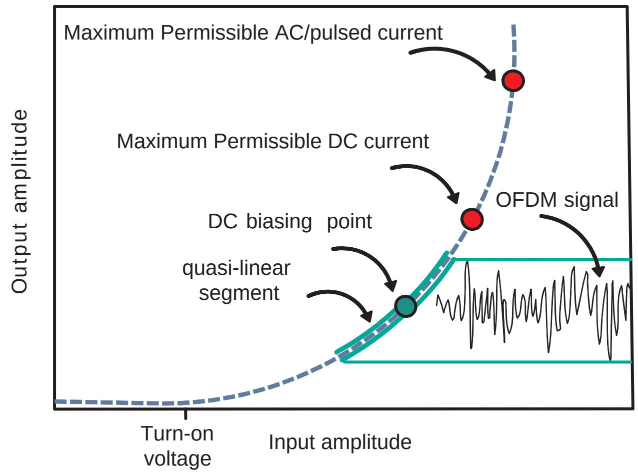

Fig. 2. Non-linear LED transfer characteristics: The typical relation between the applied forward voltage and the forward current through the LED is depicted. The non-linear transfer characteristic distorts the OFDM signal.

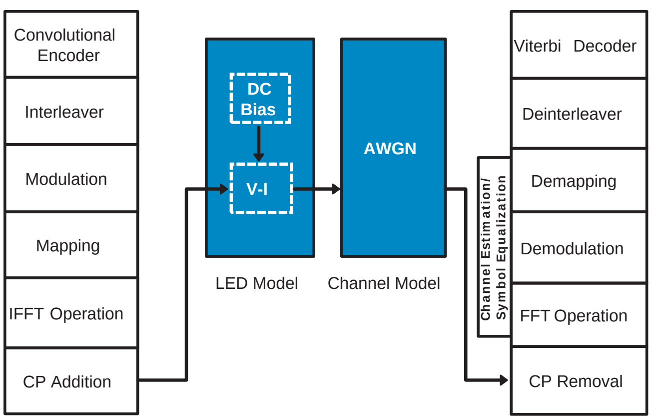

Fig. 3. The building blocks of the optical OFDM simulation model. The LED characteristics are modeled through the V-I block. The DC Bias block is used to set the LED bias point.

II. OFDM System Model

The building blocks of the implemented Matlab simulation model are shown in Fig. 3. The model continuously generates a random stream of bits. Data protection is realized through the use of forward error correction (FEC) coding (convolutional encoder) and interleaving. Different modulation schemes are considered. The generated serial stream of symbols at the modulator output is split into parallel streams, each is transmitted on a separate sub-carrier. The inverse fast Fourier transform (IFFT) operation is used to modulate the available sub-carriers and to generate the time domain OFDM signal. At the input of the IFFT, complex conjugate data symbols are used to produce a real time domain output signal as illustrated in Fig. 4.

The LED characteristic within the V-I block as shown in Fig. 3 is modeled using curve fitting techniques. The V-I block implements the relation between the forward voltage across the LED and the current through the LED. The DC bias block is used to set the bias point. In this paper, the V-I block is modeled for a high power IR LED (OSRAM, SFH

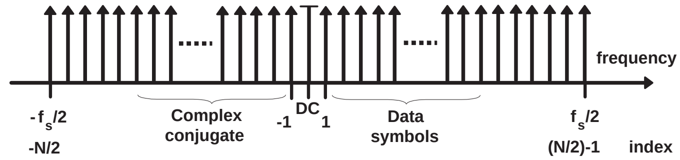

Fig. 4. IFFT bin assignment. f_s is the sampling frequency, N are the number of the IFFT bins (IFFT length, or the OFDM sub-carriers), $\frac{f_s}{2}$ is the Nyquist frequency, and the sub-carriers separation is equal to $\frac{f_s}{N}$.

4230) [15]. A least-squares curve fitting approach is used and a polynomial of the sixth degree shows the best fit for the transfer characteristic of the real LED as shown in Fig. 5. From the data sheet, the maximum permissible AC forward current is 2A. Hence, input signals producing forward current larger than 2A are clipped.

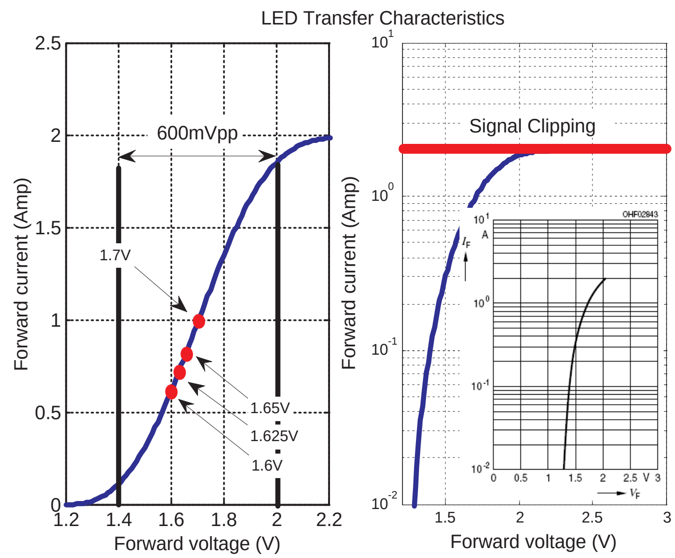

Fig. 5. The LED transfer characteristics of the OSRAM, SFH 4230 plotted using the polynomial equation describing the LED forward current and forward voltage relation. The linear scale is shown on the left curve while the semi-log scale is shown on the right curve. The curve from the data sheet is shown for comparison. The turn-on voltage is around 1.3V. The dynamic range for this particular LED is roughly around 600mVpp. The three bias points considered later on in the simulation are shown. Input signals producing forward current larger than 2Amp are clipped.

Shot noise due to background light is assumed to be the dominant source of noise and modeled as an AWGN (additive white Gaussian noise) in the simulation [16]. The OFDM demodulator implements the necessary blocks to estimate the transmitted data bits. For the purpose of channel estimation, training sequences are used [17, 18]. However, the complex conjugate requirements must be fulfilled for the OW OFDM system. Concretely, the OFDM frame is formed by four OFDM symbols for the training sequence and 20 OFDM symbols with data sub-carriers. The channel transfer factors are obtained using the training sequence and averaging over the four training sequence periods for every sub-carrier. Attaching a cyclic prefix (CP) to the transmitted

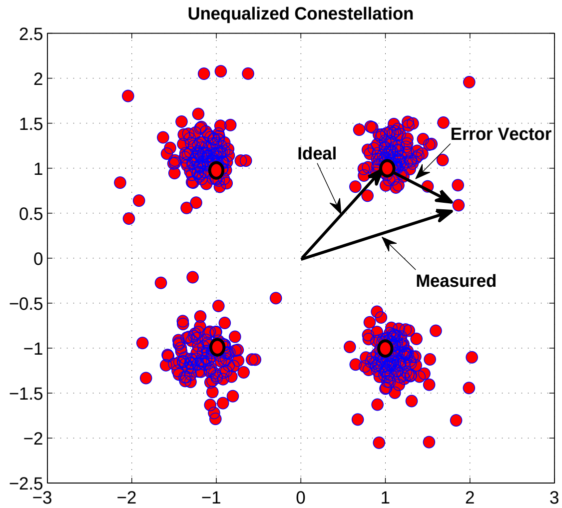

Fig. 6. A constellation diagram for a QPSK modulation with 3/4 channel coding rate with nonlinearity effects and 15dB SNR (AWGN channel without the LED generated distortion).

OFDM symbols converts the linear convolution of the channel with the OFDM signal to a circular convolution [19]. As a result, simple frequency domain equalizer can be employed. Frequency domain equalization is realized using conventional OFDM zero-forcing (ZF) detection. The equalized symbols are demodulated and the encoded symbols (a convolutional encoder is assumed at the transmitter) are decoded by the Viterbi hard-decision algorithm. The decoded bits are deinterleaved to obtain the estimated stream of data bits. In addition, the OFDM demodulator calculates the BER and the EVM used as distortion indicators in this paper.

The error vector is a common figure of merit for system linearity in digital wireless communication standards. It is a measure of the fidelity of a digital communication system and is related to in-band distortion and signal-to-noise ratio (SNR) [20]. On a constellation diagram, the error vector is a measure of the departure of signal constellation points from its ideal reference as shown in Fig. 6. The error vector is the scalar distance between the ideal constellation vector and the measured vector of the displaced constellation point after it has been compensated in timing, amplitude, frequency, phase, and DC offset. The EVM is the root mean square value of the error vector over time. To calculate the EVM, the model uses the recovered constellations to regenerate the ideal constellations. The EVM is calculated by subtracting the recovered constellations from the corresponding ideal references, taking the absolute values and calculating the RMS value over one OFDM symbol.

III. Results

From the LED data sheet, the maximum permissible DC forward current is at 1A which corresponds to 1.7V bias voltage. Therefore, five different bias points (1.6V, 1.625V, 1.65V, 1.675, and 1.7V) are considered to investigate the LED induced distortion as a function of the bias point. The distortion is characterized by the EVM in percentage. The instantaneous average power of the input OFDM signal modulating the LED is 14.5mW (calculated over one OFDM symbol). A binary phase-shift keying (BPSK) modulation scheme with 3/4 channel coding rate is used in this simulation and ideal channel is assumed (no AWGN). The EVM is computed over one OFDM symbol and the obtained values for 100 OFDM symbols are plotted in Fig. 7. Based on the obtained results, bias points of 1.6V, 1.625V, and 1.65V are considered later on in the bit-error performance and EVM investigations (as a function of power back-offs), since they achieve the lowest EVM floor, where EVM floor is defined as the lowest EVM value in a burst of 100 OFDM symbols. The OFDM and the LED simulation parameters are listed in Table I.

TABLE I
Simulation model parameters

OFDM	
IFFT length	64
Data sub-carriers	31
CP length	16 [samples]
Training symbols	4
OFDM signal power	14.5 [mW]
LED	
Biasing points	1.6/1.625/1.65 [V]
Power back-offs	0/2/4/6/8/10/12 [dB]
Signal clipping	2 [Amp]

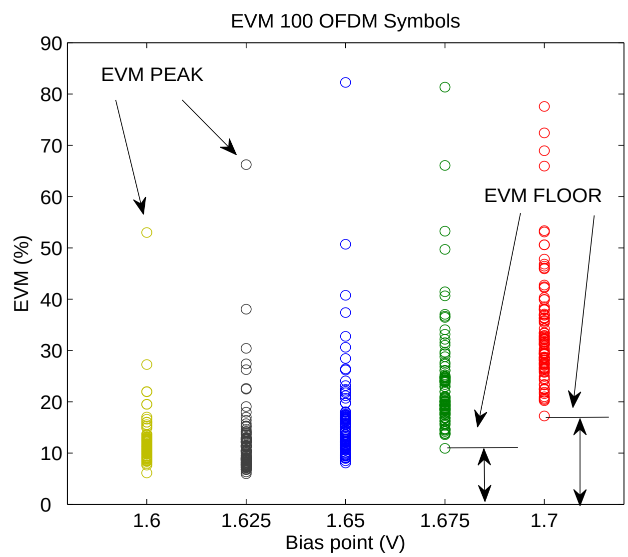

Fig. 7. The EVM scatter plot of 100 OFDM symbols versus bias point. Five different bias points (1.6V, 1.625V, 1.65V, 1.675, and 1.7V) are investigated. EVM floor is defined as the lowest EVM value in a burst of 100 OFDM symbols. EVM peak is defined as the highest EVM value in a burst of 100 OFDM symbols.

In order to study the effect of LED nonlinearity on the system performance, simulations are conducted without the LED model (only AWGN) to determine the required SNR to achieve a target BER of 10^{-5} for the three modulation schemes under investigation (BPSK, quadrature phase-shift keying (QPSK), and 16-QAM (quadrature amplitude modulation). The curves are depicted in Fig. 8 and the approximate required SNR values to achieve 10^{-5} BER are shown on the figure.

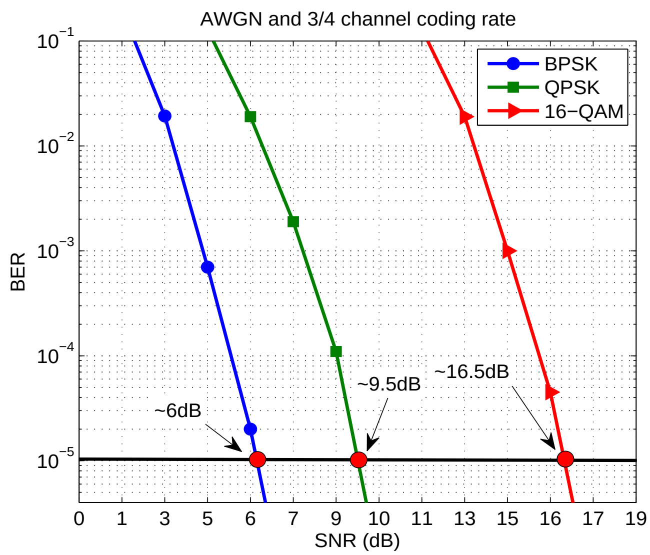

Fig. 8. BER versus SNR using AWGN channel model and 3/4 convolutional channel coding rate for BPSK, QPSK, and 16-QAM. The approximate SNR values required to achieve a target BER of 10^{-5} are 6dB, 9.5dB, and 16.5dB for BPSK, QPSK, and 16-QAM, respectively.

The BER and EVM for 1000 OFDM symbols (more than 10Mbits) are simulated at the SNR values from Fig. 8 for the three bias points and for different power back-off values. The BER and EVM simulation results for BPSK, QPSK, and 16-QAM are shown in Figs. 9, 10, and 11, respectively. In all figures, the instantaneous average power of 14.5mW is considered the 0dB power back-off. The power back-off indicates relative decrease in the input signal power and values up to 12dB are considered in the simulation.

The effect of LED nonlinearity is obvious in all figures and degradation in BER performance is noted. At 0dB power back-off, the lowest BER values achieved are 1×10^{-4}, 1×10^{-4}, and 3×10^{-3} for BPSK, QPSK, and 16-QAM, respectively. For BPSK and QPSK, BER less than 10^{-4} is achieved at 2dB power back-off while 6dB power back-off is required for the 16-QAM. The target BER of 10^{-5} can not be achieved for any of the modulation orders under investigation even with higher power back-off values. A significant observation is that for all obtained results, there is an error floor when increasing the power back-off. For instance, BER curves for BPSK and QPSK show an error floor for power back-off values larger than about 4dB. While the 16-QAM BER curve demonstrates an error floor for power back-off values larger than approximately 8dB. The error floor is a function of the bias point and depends on the EVM floor for each bias point.

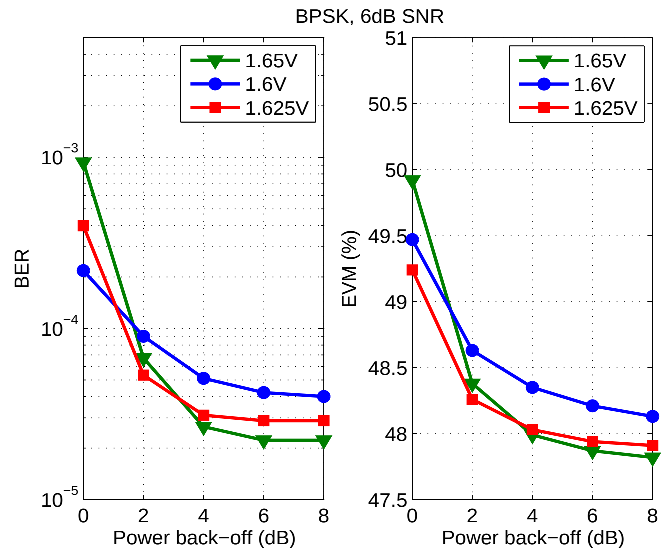

Fig. 9. The BER and EVM versus power back-offs for the three bias points under investigation. The SNR is 6dB and power back-offs up to 8dB are considered.

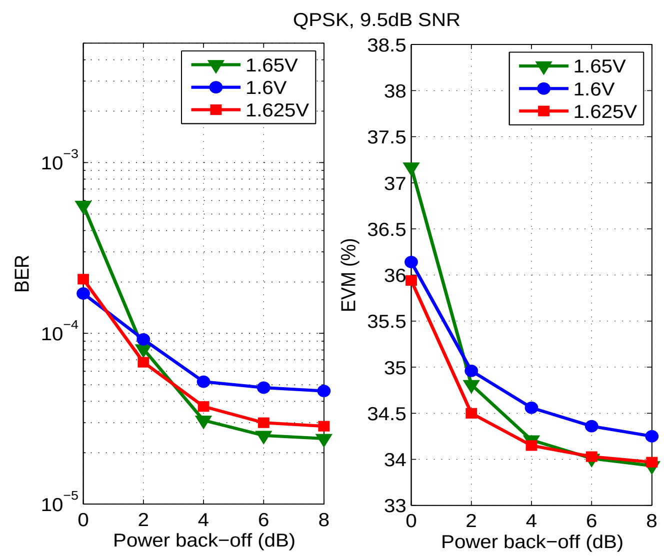

Fig. 10. The BER and EVM versus power back-offs for the three bias points under investigation. The SNR is 9.5dB and power back-offs up to 8dB are considered.

In addition, the effect of the selected bias point on the performance is noticeable in all the figures. Different bias point results in different BER and EVM performances. For the considered LED in this paper, it can be concluded that at 0dB power back-off, the 1.6V offers better bit-error performance compared to the other bias points. For example, using BPSK, 2×10^{-4} BER is achieved at 1.6V compared to 1×10^{-3} at 1.65V. Using 16-QAM, 3×10^{-3} BER is achieved at 1.6V compared to 3×10^{-2} at 1.65V. A possible reasoning is that at 1.6V, the number of clipped upper peaks of the OFDM signal is reduced. However, the 1.6V bias point demonstrates

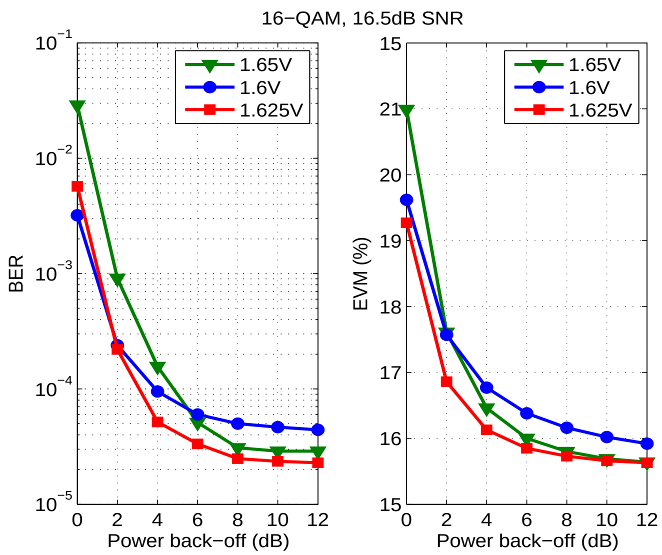

Fig. 11. The BER and EVM versus power back-offs for the three bias points under investigation. The SNR is 16.5dB and power back-offs up to 12dB are considered.

the highest distortion for power back-offs larger than 2dB and should not be considered. Therefore, and as expected, at high back-off powers, the LED operating segment of its characteristics influences the generated distortion. For power back-offs larger than 2dB, the 1.65V and the 1.625V bias points can be traded off for different modulation orders. For instance, 1.65V performers better for BPSK and QPSK modulation orders, while 1.625V shows better performance for 16-QAM.

IV. Conclusion

A model for the high power IR LED (OSRAM, SFH 4230) is considered in the simulations to study the influence of the nonlinear behavior of LEDs on the performance of OFDM based OW systems. For this particular LED (with 14.5mW OFDM signal and SNR values set to achieve 10^{-5} BER with AWGN excluding LED generated distortion), a power back-off value of 2dB is sufficient to achieve BER less than 10^{-4} for BPSK and QPSK. However, 16-QAM is more sensitive to signal distortion and requires a power back-off of 6dB to achieve BER less than 10^{-4}. At these power back-off values and/or larger values the LED can be considered operating in a quasi-linear segment of its characteristic for the three bias points and the three modulation orders under investigation.

The optical link can be maintained using low order modulation schemes (BPSK and QPSK) even with high signal deterioration. For example, BPSK modulation using 3/4 channel coding rate achieves 2×10^{-4} BER at 49.5% EVM (6dB SNR, 1.6V bias point, and 0dB back-off power). It is also shown that higher modulation schemes such as the 16-QAM are very sensitive to the operating bias point. The 16-QAM modulation using 3/4 channel coding rate achieves 3×10^{-3} BER at 1.6V and 2×10^{-2} at 1.65V (16.5dB SNR and 0dB power back-off).

In a practical system, the bias point should be adjusted depending on the power back-off and the modulation order, and this should be done dynamically when using adaptive modulation techniques.

References

[1] IEEE Standards Association (IEEE-SA), retrieved Jun. 2008 http://standards.ieee.org.

[2] D. Dardari, V. Tralli, and A. Vaccari, "A Theoretical Characterization of Nonlinear Distortion Effects in OFDM Systems," *IEEE Transactions on Communications*, vol. 48, no. 10, pp. 1755–1764, Oct. 2000.

[3] X. Li and J. Cimini, L.J., "Effects of Clipping and Filtering on the Performance of OFDM," *IEEE Communications Letters*, vol. 2, no. 5, pp. 131–133, May 1998.

[4] A. Bahai, M. Singh, A. Goldsmith, and B. Saltzberg, "A New Approach for Evaluating Clipping Distortion in Multicarrier Systems," *IEEE Journal on Selected Areas in Communications*, vol. 20, no. 5, pp. 1037–1046, Jun. 2002.

[5] Y. Li and G. Stüber, Eds., *Orthogonal Frequency Division Multiplexing for Wireless Communications*. Springer, 2006.

[6] T. Pratt, N. Jones, L. Smee, and M. Torrey, "OFDM Link Performance with Companding for PAPR Reduction in the Presence of Non-linear Amplification," *IEEE Transactions on Broadcasting*, vol. 52, no. 2, pp. 261–267, 2006.

[7] V. Ahirwar and S. Rajan, "Tradeoff between PAPR Reduction and Decoding Complexity in Transformed OFDM Systems," in *Proc. of the International Symposium on Information Theory (ISIT)*, Sep. 4–9, 2005, pp. 1256–1260.

[8] D. Wulich and G. Tsouri, "Is PAPR reduction always justified for OFDM?" in *Proc. of the 13th European Wireless Conference (EW)*, Paris, France, Apr. 1–4, 2007.

[9] T. Komine and M. Nakagawa, "Fundamental Analysis for Visible–Light Communication System using LED Lights," *IEEE Transactions on Consumer Electronics*, vol. 50, no. 1, pp. 100–107, Feb. 2004.

[10] J.-H. Kim, C. G. Lee, C. S. Park, S. Hann, and D.-H. Kim, "Visible Light Communication at 20 Mb/s Using Illumination LEDs," in *Proc. SPIE*, vol. 6353, no. 40, Gwangju, South Korea, Sep. 5, 2006.

[11] Y. Tanaka, T. Komine, S. Haruyama, and M. Nakagawa, "Indoor Visible Communication Utilizing Plural White LEDs as Lighting," in *Proc. of the 12th IEEE International Symposium on Personal, Indoor and Mobile Radio Communications*, vol. 2, San Diego, CA, USA, Sep. 30 – Oct. 3, 2001, pp. 81–85.

[12] M. Z. Afgani, H. Haas, H. Elgala, and D. Knipp, "Visible Light Communication Using OFDM," in *Proc. of the 2nd International Conference on Testbeds and Research Infrastructures for the Development of Networks and Communities (TRIDENTCOM)*, Barcelona, Spain, Mar. 1–3, 2006, pp. 129–134.

[13] H. Elgala, R. Mesleh, H. Haas, and B. Pricope, "OFDM Visible Light Wireless Communication Based on White LEDs," in *Proc. of the 64th IEEE Vehicular Technology Conference (VTC)*, Dublin, Ireland, Apr. 22–25, 2007.

[14] O. Gonzalez, R. Perez-Jimenez, S. Rodriguez, J. Rabadan, and A. Ayala, "OFDM Over Indoor Wireless Optical Channel," *Optoelectronics, IEE Proceedings*, vol. 152, no. 4, pp. 199–204, Aug. 2005.

[15] OSRAM GmbH, "Datasheet: SFH 4230 High Power Infrared Emitter," Retrieved from http://www.osram.de, Mar. 2008.

[16] J. B. Carruthers and J. M. Kahn, "Modeling of Nondirected Wireless Infrared Channels," in *Proc. of the IEEE Conference on Communications.: Converging Technologies for Tomorrow's Applications*, vol. 2, Dallas, TX, USA, Jun. 23–27, 1996, pp. 1227–1231.

[17] P. Moose, "A Technique for Orthogonal Frequency Division Multiplexing Frequency Offset Correction," *IEEE Transactions on Communications*, vol. 42, no. 10, pp. 2908–2914, Oct. 1994.

[18] H. Tang, K. Lau, and R. Brodersen, "Synchronization schemes for packet OFDM system," in *Proc. of the IEEE International Conference on Communications (ICC 03)*, vol. 5, May 11–15, 2003, pp. 3346–3350.

[19] J. G. Andrews, A. Ghosh, and R. Muhamed, *Fundamentals of WiMAX*. Pearson Education, Inc., 2007.

[20] K. Gharaibeh, K. Gard, and M. Steer, "Accurate Estimation of Digital Communication System Metrics - SNR, EVM and ρ in a Nonlinear Amplifier Environment," in *Proc. of the 64th ARFTG Conference on Microwave Measurements*, Orlando, Florida,USA, Dec. 2–3, 2004, pp. 41–44.